


RESEARCH

Open Access



# Can a fast T2-Dixon sequence surpass the time obstacle of whole-body MRI in the evaluation of skeletal metastases?

Mostafa Elmansy<sup>1\*</sup> , Noha Magdi<sup>1</sup>, Mohammed A. Elhawary<sup>1</sup> and Amina Sultan<sup>1</sup>

## Abstract

**Background** Whole-body magnetic resonance imaging (WB-MRI) has shown its accuracy in the diagnosis of skeletal metastases in patients with known primary solid cancers. The standard protocol was a combination of T1 and short tau inversion recovery (STIR) sequences. Herein, this study was conducted to elucidate the role of the T2-Dixon sequence as a rapid alternative to the standard protocol with the assessment of its diagnostic accuracy and comparability to the established methodology.

**Methods** This prospective study included 30 patients with primary solid malignancies who underwent WB-MRI. The sequences obtained were T1WI, STIR, and T2-Dixon (fat-only and water-only images). Skeletal metastases were evaluated in each sequence. Results were compared between the T1-STIR combination and T2-Dixon fat and water reconstructions.

**Results** The sensitivity of fat and water reconstructions from a single T2-Dixon in the detection of lytic skeletal metastases was marginally superior to a combination of T1WI and STIR sequences (0–7%). Detection of mixed lesions demonstrated equally high sensitivity in both protocols. Sclerotic metastases detection in WB-MRI showed low sensitivity in both protocols. However, specificity surpassed 95% for all lesion types in both protocols. Overall image quality was favored (in 87–90% of patients) in T2-Dixon images. The overall estimated acquisition timing using T2-Dixon appeared to be approximately half that of the standard T1-STIR combination.

**Conclusions** WB-MRI using T2-Dixon fat and water reconstructions showed similar accuracy to T1WI and STIR combination in the evaluation of skeletal metastases in patients with primary solid cancers with significantly shorter acquisition time.

**Keywords** Whole-body magnetic resonance imaging, T2-Dixon sequence, Skeletal metastases, T1WI and STIR sequences

## Background

Bone metastases are most common in patients with advanced stages of breast, prostate, lung, and thyroid cancers leading to pain and pathological fractures, which

significantly lower the quality of life. Additionally, they are minor contributors to gastrointestinal and uterine cancers [1].

Clinical guidelines now recommend whole-body magnetic resonance imaging (WB-MRI) for skeletal lesion detection and follow-up in patients with metastases from solid tumors due to its outstanding diagnostic performance in recent years [2–6].

In routine whole-body magnetic resonance imaging (WB-MRI) examinations, anatomical T1WI and

\*Correspondence:

Mostafa Elmansy  
mostafaelmansy@mans.edu.eg

<sup>1</sup> Department of Radiology, Mansoura University Hospitals, Mansoura, Egypt

short-tau inversion recovery (STIR) sequences are integrated with functional diffusion-weighted imaging (DWI) sequences. The inclusion of STIR images enhances sensitivity in detecting lesions, while the T1WI sequence functions as the reference for characterizing and detecting marrow lesions. The incorporation of DWI sequences, owing to their high contrast between lesions and background tissues, expands the scope of cancer screening to include lymph nodes and extra-skeletal organs, thereby augmenting the diagnostic utility of the anatomical sequences [7–9].

As the two main barriers preventing WB-MRI from being used widely are cost and lengthy scan times, it's critical to maximize diagnostic value while minimizing acquisition time, especially for cancer patients who might be in pain or fragile [10, 11].

The Dixon technique depends on the chemical shift between water and fat. Four types of images can be obtained from a single T2 Dixon sequence, which are: in-phase (IP) (equivalent to non-fat suppressed anatomic images), out-of-phase (OP), water images (equivalent to fat-suppressed), and fat images (equivalent to water-suppressed). Therefore, the Dixon technique, when applied correctly, can obtain T1-weighted and STIR-like pictures in little scan times [11, 12].

In this study, we aimed to investigate if neoplastic bone marrow lesions can be detected with good diagnostic accuracy using a faster WB-MRI protocol that uses a single T2 Dixon sequence. Comparing combined fat + water reconstructions from a single T2 Dixon sequence to the standard T1WI and STIR sequences will be the primary method used to assess our hypothesis.

## Methods

### Patient population

From February 2023 to February 2024, our prospective study involved 30 adult patients (20 women, age range of 36–74 years, mean age of 55.6 years; 10 men, age range of 44–77 years; mean age of 63 years). Inclusion criteria were patients with solid cancers who had a high risk of metastases and underwent post-contrast whole-body computed tomography study which resulted in suspected or definite bone metastases. Half of the patients were diagnosed with breast cancer, the rest were diagnosed with other variable malignancies, including prostate, colon, lung, laryngeal, renal, gastric, ovarian cancers, and non-Hodgkin lymphoma. They all had informed consent before the whole-body MRI examination. CT imaging was performed within 4 weeks before the whole-body MRI.

Patients who had received treatment or had multiple malignancies were excluded. Other exclusion

criteria included MRI contraindications as claustrophobic patients.

### MRI protocol

Whole-body MRI was performed on a 1.5-T Siemens Magnetom Aera. Imaging was done head first in the supine position, from head to proximal femurs, covered with body, brain, and three body matrix coils. The sequences obtained were T1WI, STIR, and DWI, and the four images were automatically acquired from the T2 Dixon sequence (fat only, water only, IP, and OP). Imaging was done in four stacks of T1WI, STIR, and T2 Dixon in the coronal plane and five stacks of DWI in the axial plane. After that, a single reformatted stack of the whole body is reconstructed in each sequence. Detailed imaging parameters are shown in Table 1.

### Interpretation of MRI imaging

Eight skeletal regions including femurs, pelvis, lumber vertebrae, thoracic vertebrae, cervical vertebrae, thoracic cage, humeri, and skull were assessed in our study. Normal marrow signal was defined as a homogenous high signal in T1WI and fat images and a homogenous low signal in STIR and water images.

Based on well-defined criteria, the bone marrow lesion in each region was classified as either lytic, sclerotic, or mixed lesion. The lytic lesion was defined as a low signal of bone marrow in T1WI images and Dixon fat images (similar to the disc signal or lower) and an intermediate to high signal in STIR and water images [12]. The sclerotic lesion was defined as a darker signal than yellow marrow and slightly darker or isointense to red marrow. On STIR and water images, these were minimally brighter than both red and yellow marrow and may be surrounded by a rim of hyperintense signal [13, 14]. The mixed lesion was considered a combination of the two patterns. The lesions are counted per-regionally according to the following numerical code: 0 = no lesions; 1 = 1–5 lesions; 2 = 6–10 lesions; 3 = more than 10 lesions; 4 = diffuse disease.

Two junior and senior radiologists with 2 years and 9 years of experience respectively reviewed the sequences and were blinded to the clinical data. During single separate sessions, the two radiologists made both semiquantitative and qualitative analyses of T2-Dixon water-only images in comparison with STIR images on a per-patient basis. Likewise, the analyses of T2-Dixon fat-only images were compared to T1-weighted images. Regarding the image quality assessment, evaluation criteria included overall image quality, motion artifact, anatomical sharpness, CSF flow artifact, and fat suppression in fat-suppressed images. The images were juxtaposed, and the optimal quality or least artifact in each category was chosen.

**Table 1** Our imaging parameters of each sequence used in WB-MRI examination in our study

Parameter	2D T1 FSE	STIR	T2 Dixon	DWI
Scan orientation	Coronal	Coronal	Coronal	Axial
Phase-encoding direction	Right–left	Right–left	Right–left	Posterior–anterior
Voxel size (mm) (read×phase×slice)	1.3×1.3×6	0.8×0.8×6	1.3×1.3×6	1.7×1.7×4.5
Field of view (read) (mm)	410	400	400	440
Field of view (phase) (%)	112.5	112.5	112.5	65.6
Slice thickness	6	6	6	4.5
No. of stations	4	4	4	5
Phase oversampling (%)	25%	50%	0%	0%
TR/TE (ms)	800/7.7	3300/84	1550/106	7010/50
T1 (ms)	–	180	–	180
Turbo factor	11	–	23	–
Bandwidth (Hz)	319	543	625	1562
Fat suppression technique	None	STIR	Dixon	SPAIR
<i>b</i> values, s/mm <sup>2</sup>	–	–	–	800
Acquisition time, per stack	2 min 34 s	52 s	1 min 42 s	1 min 31 s
Total acquisition time, per sequence	10 min 16 s	3 min 28 s	6 min 48 s	6 min 4 s

FSE fast spin-echo, STIR short-T1 inversion recovery sequence, DWI diffusion-weighted imaging sequence, TR repetition time, TE echo time, T1 inversion time

Interreader reliability was done between both junior and senior readers. All the images included in the study were read and stored on the Picture Archiving and Communication System (PACS). DWI was reviewed only in the consensus session to establish the gold standard.

### Reference standard

The reference standard in our study was established during a consensus session involving the two main junior and senior readers with two other experts in musculoskeletal radiology having experience of 12 years and 30 years respectively. The decision was made based on clinical data, and different previous and follow-up imaging modalities including (T1WI, STIR, fat and water reconstructed images from T2 Dixon, and DW MR sequences) in all patients, whole body computed tomography in all patients, positron emission tomography (PET-CT), and nuclear medicine bone scans when were available.

### Statistical analysis

Data was entered and analyzed using IBM-SPSS software. Inter-reader agreement between senior and junior readers was assessed using Weighted kappa ( $\kappa_w$ ). The strength of inter-reader agreement was interpreted according to guidelines from Altman, and adapted from Landis and Koch:  $\kappa_w < 0.20$  = poor;  $0.21 \leq \kappa_w < 0.40$  = fair;  $0.41 \leq \kappa_w < 0.60$  = moderate;  $0.61 \leq \kappa_w < 0.80$  = good;  $\kappa_w \geq 0.81$  = very good and  $\kappa_w = 1$  = perfect [15, 16].

Diagnostic accuracy and agreement between each protocol and the reference standard were measured using Online Confusion matrix software. True positives (TP),

false positives (FP), false negatives (FN), true negatives (TN), sensitivity (Se), specificity (Sp), accuracy, Matthews Correlation Coefficient (MCC), and  $\kappa_w$  were reported for the per-region analyses (for both readers).

### Results

Regarding the lesions detected in our sample, twenty patients were found to have focal marrow lesions, six patients had diffuse marrow lesions and four patients had normal marrow. The number of focal marrow lesions couldn't be accurately counted as we depended on a semi-quantitative score (the numerical code). However, there were at least 27,86, 38, 37, 16, 19, 9, and 1 lesions in femurs, pelvis, lumber, dorsal, cervical spine, thoracic cage, humeri, and skull respectively. There was a count of at least 111 lytic lesions, 55 sclerotic lesions, and 71 mixed lesions. Totally, there were at least 237 focal marrow lesions detected in the study. Diffuse marrow lesions were detected 24 times in the study in different regions and they were all of mixed nature. The majority of the lesions depicted in our patient sample were found to be lytic and focal. Per-regionally, the highest metastases burden was detected at the pelvis, lumber, and dorsal vertebrae respectively. Numerical details are summarized in Fig. 1.

T2-Dixon showed better sensitivity than T1/STIR regarding lytic lesions and similar sensitivity and specificity regarding mixed and sclerotic lesions. It depicted a sensitivity of more than 89% for both junior and senior readers and a specificity of more than 95% for both readers as well in lytic lesion detection. The sensitivity

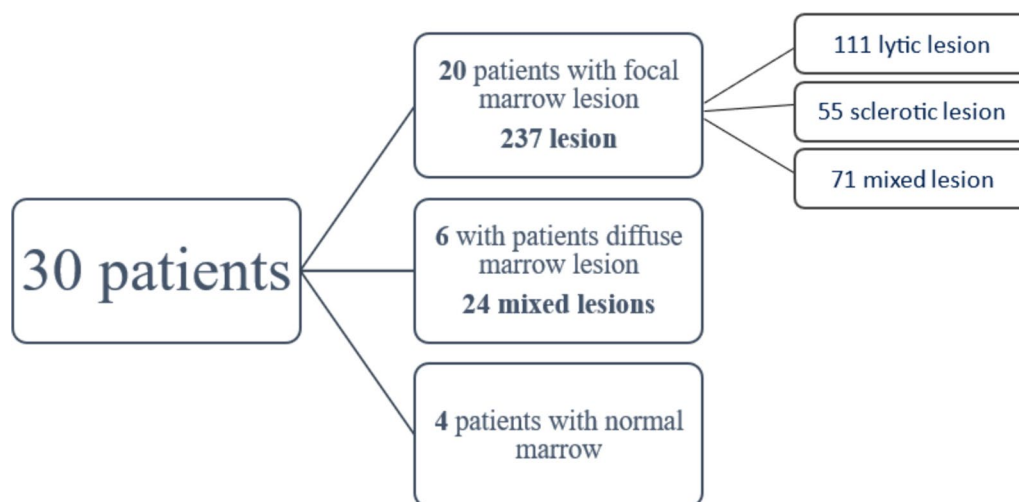


**Fig. 1** The least number of each type of lesions detected in the study and their distribution pattern in the study sample

of T2 Dixon in mixed lesions was more than 80% with a specificity of 100% for both readers. Our results were highly variable and not conclusive regarding the sensitivity of sclerotic lesion detection. Despite the variability, T2-dixon showed higher sensitivity than T1/STIR in some regions (the pelvis, lumbar and thoracic vertebrae). However, regarding the specificity of sclerotic lesion detection, T1 + STIR and T2 Dixon showed 100% specificity for both senior and junior readers. The diagnostic characteristics and agreement between the protocols and the reference standard are demonstrated in Table 2. The sensitivity and specificity of our imaging sequences are summarized in Table 3.

Regarding the regions, the lowest accuracy in detecting lesions was observed in thoracic cage and cervical vertebrae, with Dixon outperforming T1/STIR in these areas. Conversely, the highest accuracy was exhibited in the femurs and pelvis. The evaluation of lesions in the humeri and skull was constrained by the small number of lesions in the study. Detailed sensitivity and specificity of each reader per region are listed in Supplement Table 1. Agreement between different imaging modalities and different MRI sequences in some of our cases is shown in Figs. 2, 3 and 4.

In the context of image quality, the T2-Dixon images demonstrated less motion artifact, better anatomic sharpness, and less CSF flow artifact by the two readers. There was no significant difference in the homogeneity of fat suppression between STIR and T2-Dixon water images. For overall image quality, the T2-Dixon fat images were preferred in 87% of patients and T2-Dixon water images were chosen in 90% of patients. The detailed results of image quality evaluation are listed in Table 4.

Regarding the inter-reader agreement, there was perfect to very good agreement between the junior and senior readers regardless of the region in both standard T1 + STIR and Dixon T2 fat + water. The agreement was measured using Weighted kappa [15]. All values showed perfect agreement ( $K_w = 1$ ) with some exceptions listed in Table 5.

## Discussion

In the realm of oncology, accurate staging is crucial for effective treatment planning, especially in cases where bone metastases are prevalent, such as in breast cancer. Recent advancements in imaging technology, particularly whole-body MRI (WB-MRI), offer a comprehensive view of metastatic spread, encompassing skeletal and soft tissue organs, while avoiding radiation hazards [7]. Our study aimed to evaluate the feasibility of integrating the T2-Dixon sequence into oncology scanning protocols as a simplified and faster alternative to standard sequences. We assessed its diagnostic accuracy, compared it with the conventional T1WI and STIR protocols, and evaluated its ability to detect various lesion types (lytic, sclerotic, and mixed). Additionally, we examined the image quality of the T2-Dixon sequence and explored the possibility of reducing acquisition time while maintaining diagnostic accuracy.

Our study has proven the feasibility of employing the T2-Dixon sequence as an expeditious substitute for the conventional T1WI and STIR combination in the scanning protocol for oncology patients to detect bone metastases with good comparable sensitivity and specificity to the conventional T1-STIR WB-MRI protocol. Additionally, T2-dixon images showed better overall image quality and fewer artifacts when assessed in each

**Table 2** Diagnostic characteristics and agreement between the protocols and the reference standard in the whole cohort of patients (N = 30)

	TP	FP	FN	TN	Se	Sp	PPV	NPV	ACC	F1	MSS	Weighted kappa		
												k <sub>w</sub>	95% CI	Agreement
<i>Standard (T1, STIR)</i>														
Femurs														
Lytic	7	0	0	23	1	1	1	1	1	1	1	1	1–1	Perfect
Sclerotic	2	0	0	28	1	1	1	1	1	1	1	1	1–1	Perfect
Mixed	5	0	0	25	1	1	1	1	1	1	1	1	1–1	Perfect
Pelvis														
Lytic	10	0	0	20	1	1	1	1	1	1	1	0.96	0.89–1	Very good
Sclerotic	2	0	1	27	0.67	1	–	0.96	0.97	0.8	0.8	0.82	0.6–1	Very good
Mixed	9	0	0	21	1	1	1	1	1	1	1	1	1–1	Perfect
Lumber v														
Lytic	8	0	1	21	0.89	1	–	0.96	0.97	0.94	0.92	0.94	0.81–1	Very good
Sclerotic	2	0	1	27	0.67	1	–	0.96	0.97	0.8	0.8	0.85	0.53–1	Very good
Mixed	7	0	0	23	1	1	1	1	1	1	1	1	1–1	Perfect
Thoracic v														
Lytic	9	1	2	18	0.82	0.95	–	0.9	0.9	0.86	0.78	0.81	0.6–1	Very good
Sclerotic	3	0	1	26	0.75	1	–	0.96	0.97	0.86	0.85	0.9	0.69–1	Very good
Mixed	8	0	0	28	1	1	1	1	1	1	1	1	1–1	Perfect
Cervical v														
Lytic	2	0	0	28	1	1	1	1	1	1	1	1	1–1	Perfect
Sclerotic	1	0	2	27	0.33	1	–	0.93	0.93	0.50	0.56	0.38	–0.001–0.75	Fair
Mixed	4	0	1	25	0.8	1	–	0.96	0.97	0.89	0.88	0.77	0.49–1	Good
Thoracic cage														
Lytic	5	0	3	22	0.63	1	1	0.88	0.9	0.77	0.74	0.71	0.41–1	Good
Sclerotic	0	0	5	25	0	1	–	0.83	0.83	0	–	0	0–0	Poor
Mixed	6	0	0	24	1	1	1	1	1	1	1	1	1–1	Perfect
Humeri														
Lytic	4	0	0	26	1	1	1	1	1	1	1	1	1–1	Perfect
Sclerotic	0	0	2	28	0	1	–	0.93	0.93	0	–	0	0–0	Poor
Mixed	4	0	0	26	1	1	1	1	1	1	1	1	1–1	Perfect
Skull														
Lytic	–	–	–	–	–	–	–	–	–	–	–	–	–	–
Sclerotic	–	–	–	–	–	–	–	–	–	–	–	0	0–0	–
Mixed	1	0	0	29	1	1	1	1	1	1	1	1	1–1	Perfect
<i>Dixon (Fat + water)</i>														
Femurs														
Lytic	7	0	0	23	1	1	1	1	1	1	1	1	1–1	Perfect
Sclerotic	2	0	0	28	1	1	1	1	1	1	1	1	1–1	Perfect
Mixed	5	0	0	25	1	1	1	1	1	1	1	1	1–1	Perfect
Pelvis														
Lytic	10	0	0	20	1	1	1	1	1	1	1	0.93	0.79–1	Very good
Sclerotic	3	0	0	27	1	1	1	1	1	1	1	0.92	0.79–1	Very good
Mixed	9	0	0	21	1	1	1	1	1	1	1	1	1–1	Perfect
Lumber v														
Lytic	8	1	1	20	0.89	0.95	–	0.95	0.93	0.89	0.84	0.88	0.71–1	Very good
Sclerotic	3	0	0	27	1	1	1	1	1	1	1	1	1–1	Perfect
Mixed	7	0	0	23	1	1	1	1	1	1	1	1	1–1	Perfect
Thoracic v														

**Table 2** (continued)

	TP	FP	FN	TN	Se	Sp	PPV	NPV	ACC	F1	MSS	Weighted kappa		
												k <sub>w</sub>	95% CI	Agreement
Lytic	11	0	0	19	1	1	1	1	1	1	1	1	1–1	Perfect
Sclerotic	4	0	0	26	1	1	1	1	1	1	1	1	1–1	Perfect
Mixed	8	0	0	22	1	1	1	1	1	1	1	1	1–1	Perfect
Cervical v														
Lytic	2	0	0	28	1	1	1	1	1	1	1	1	1–1	Perfect
Sclerotic	1	0	2	27	0.33	1	–	0.93	0.93	0.50	0.56	0.38	–0.001–0.75	moderate
Mixed	4	0	1	25	0.8	1	–	0.96	0.97	0.89	0.88	0.77	0.49–1	Good
Thoracic cage														
Lytic	8	0	0	22	1	1	1	1	1	1	1	1	1–1	Perfect
Sclerotic	0	0	5	25	0	1	–	0.83	0.83	0	–	0	0–0	Poor
Mixed	6	0	0	24	1	1	1	1	1	1	1	1	1–1	Perfect
Humeri														
Lytic	4	0	0	26	1	1	1	1	1	1	1	0.87	0.69–1	Very good
Sclerotic	0	0	2	28	0	1	–	0.93	0.93	0	–	0	0–0	Poor
Mixed	4	0	0	26	1	1	1	1	1	1	1	1	1–1	Perfect
Skull														
Lytic	–	–	–	–	–	–	–	–	–	–	–	–	–	–
Sclerotic	–	–	–	–	–	–	–	–	–	–	–	0	0–0	–
Mixed	1	0	0	29	1	1	1	1	1	1	1	1	1–1	Perfect

TP true positive, FP false positive, FN false negative, TN true negative, Se sensitivity, Sp specificity, PPV positive predictive value, NPV negative predictive value, ACC accuracy, MSS Matthews correlation coefficient, K<sub>w</sub> weighted kappa, CI confidence interval

**Table 3** The summarized sensitivity and specificity of T1/STIR and T2 Dixon (fat + water)

	Sensitivity R1 (%)	Sensitivity R2 (%)	Specificity R1 (%)	Specificity R2 (%)
T1 + STIR				
Lytic	75–100	82–100	89–100	95–100
Sclerotic	0–75	0–75	100	100
Mixed	80–100	80–100	100	100
Dixon (fat + water)				
Lytic	89–100	89–100	95–100	95–100
Sclerotic	0–100	0–100	100	100
Mixed	80–100	80–100	100	100

(See figure on next page.)

**Fig. 2** The agreement between different modalities in bone metastases detection in a 71-year-old male patient diagnosed with non-Hodgkin lymphoma, **a** T2-Dixon fat image shows two focal osseous lesions in both iliac bones, **b** T2-Dixon water image correlation, **c** STIR image correlation, **d** T1WI image, **e** and **f** 18-FDG PET-CT image correlation showing tracer uptake in the same regions. The reference standard confirmed the presence of these lesions. It is noticeable that overall image quality and contrast-to-noise ratio are better in T2-Dixon images in comparison with T1WI and STIR images

patient separately compared to the standard T1WI and STIR sequences.

Some previously published studies compared the two protocols in certain regions such as the spine only [17]

or the whole body regardless of the type of lesion. Previous studies showed similar accuracy between both protocols [12, 18]. To the best of our knowledge, our study was the first to particularly analyze metastatic bony lesions according to their type whether lytic,

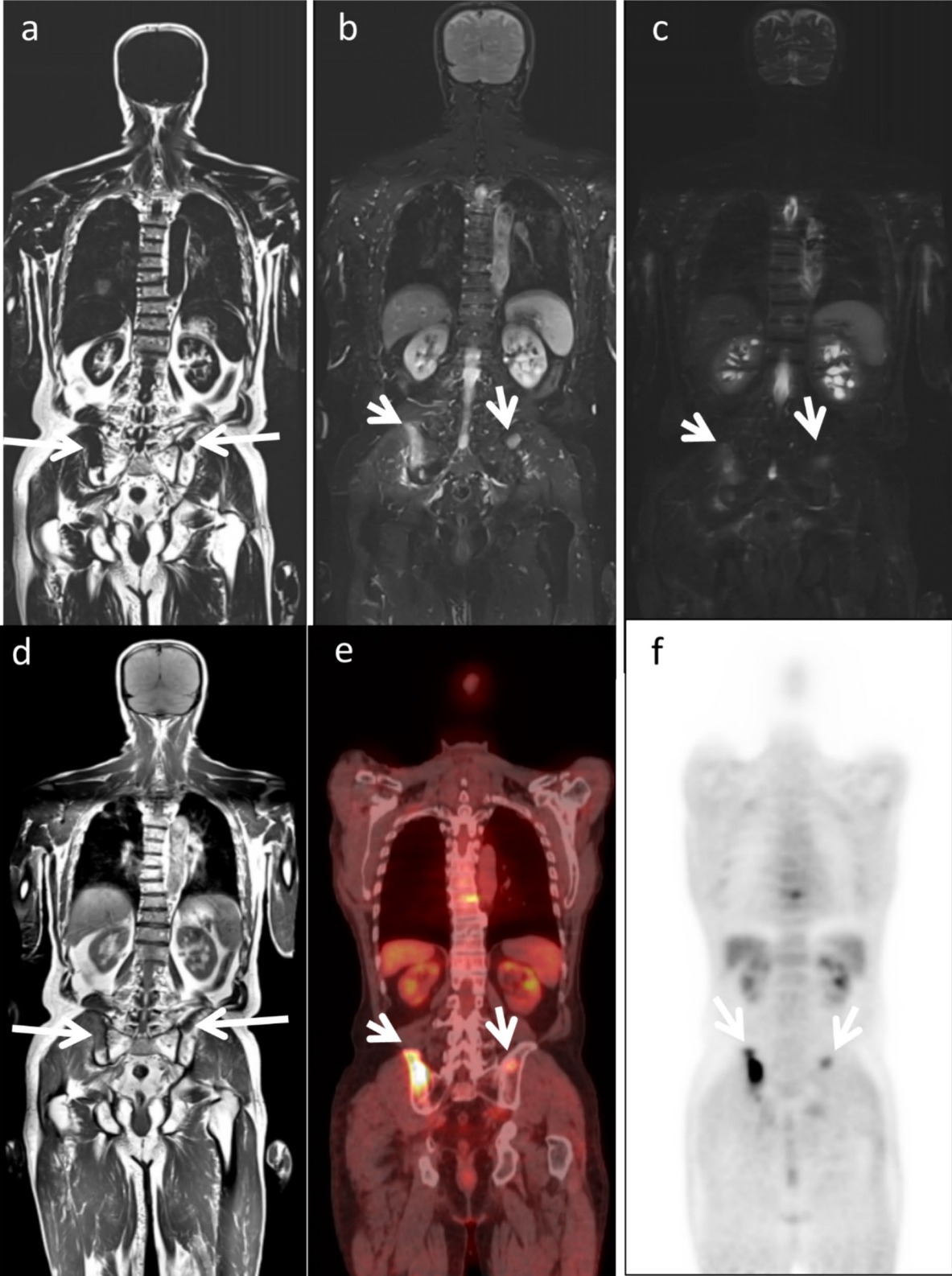
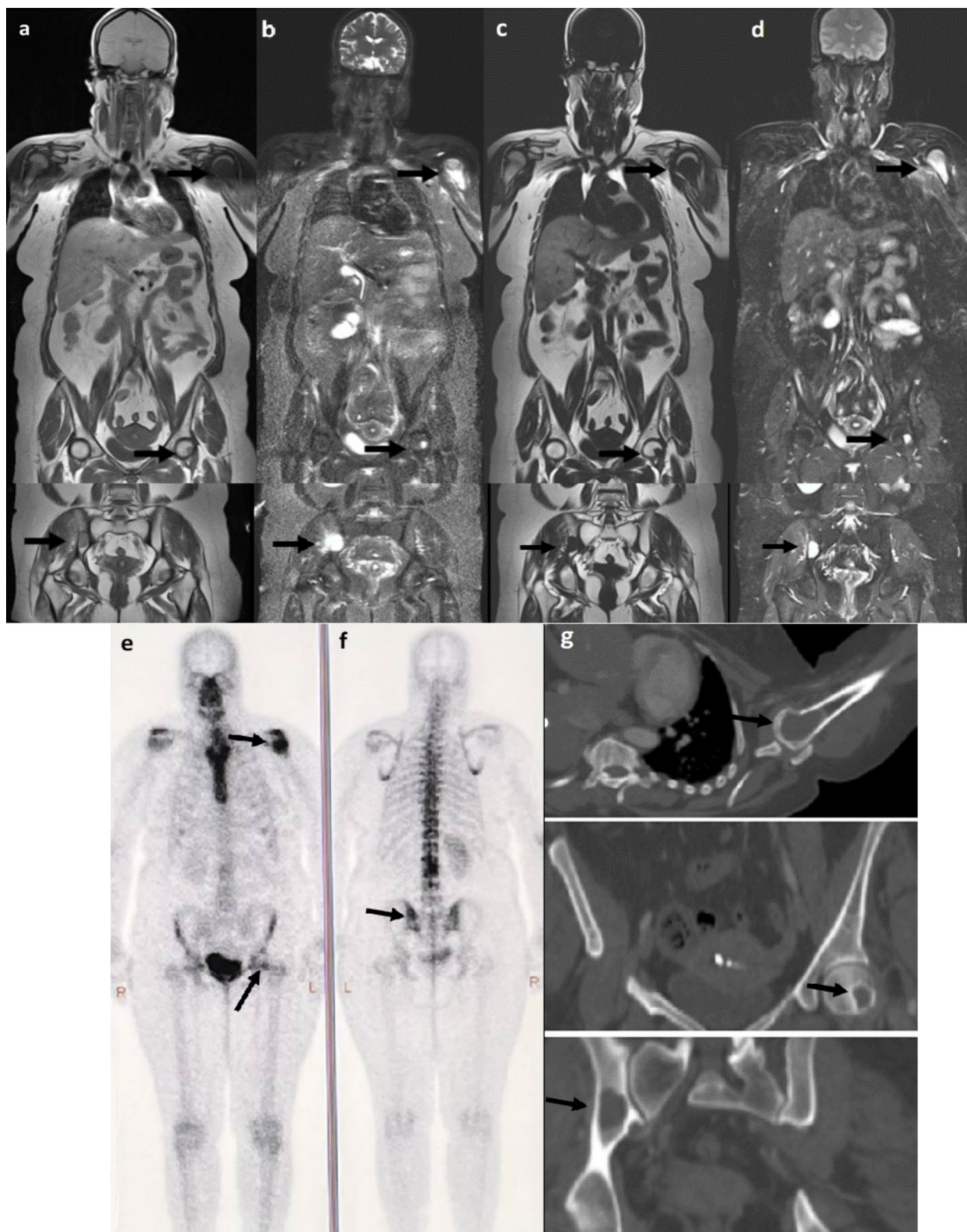
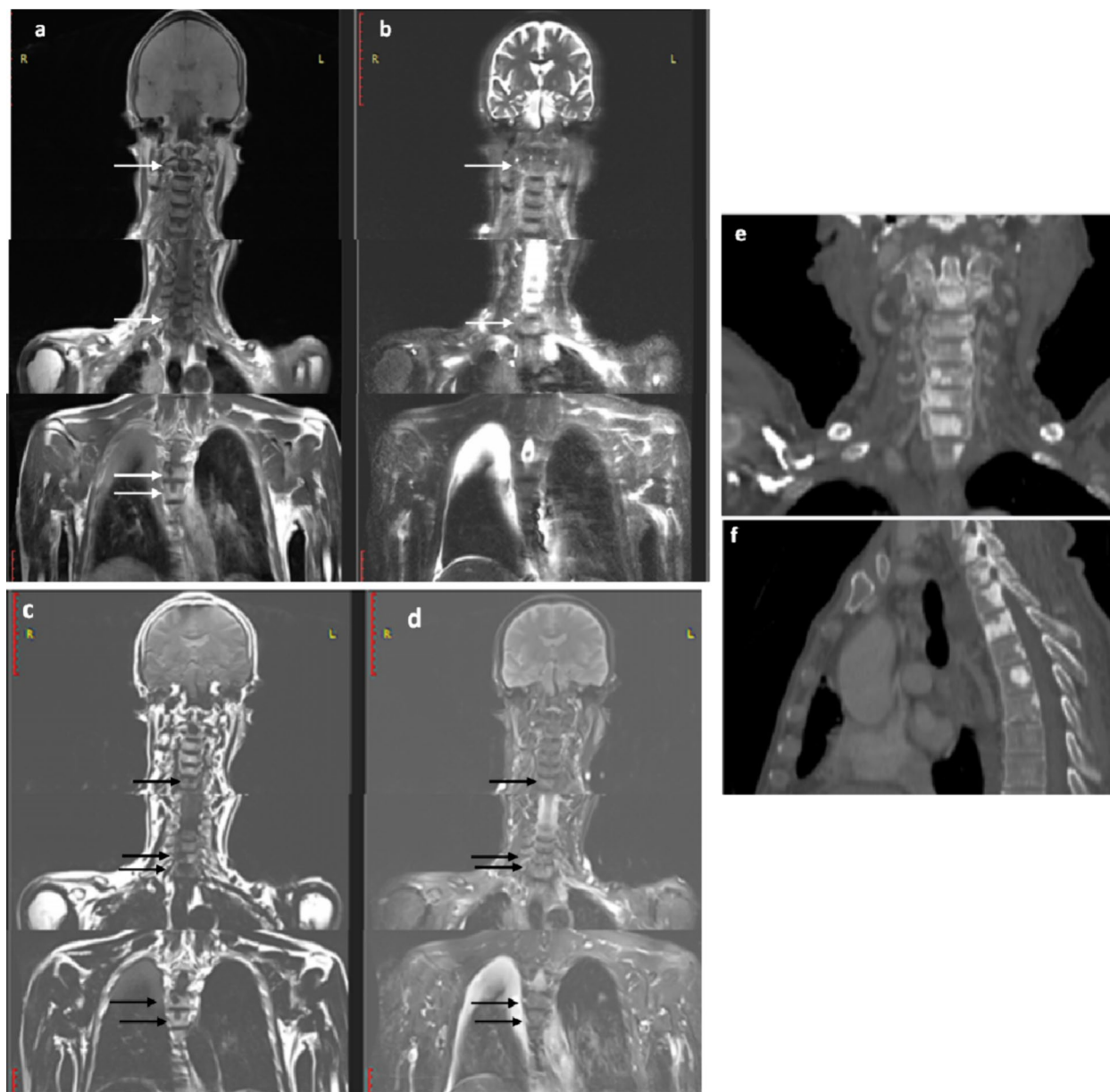


Fig. 2 (See legend on previous page.)



**Fig. 3** Bone metastases in a 47-year-old female patient with a history of operated left renal cell carcinoma, underwent an MRI which showed lesions of abnormal SI at the left humeral head, left femoral head, and right iliac bone in the following sequences **a** coronal whole body T1WI, **b** STIR, **c** Dixon-fat only image, and **d** Dixon-water only images respectively, **e** and **f** whole views body scan showed foci of increased radioactive tracer uptake at the same three sites, **g** oblique and two coronal CT images showed lytic lesions at the same sites





**Fig. 4** Multiple focal sclerotic osseous metastases in a case of breast cancer **a** coronal whole body T1WI, **b** STIR, **c** Dixon-fat only image, and **d** Dixon-water only image respectively showed lesions of abnormal SI in the form of low signal in both T1WI and Dixon fat only images and slightly low signal with hyperintense rim in STIR and Dixon water only images at cervical and thoracic vertebrae, **e** and **f** CT images demonstrated multiple sclerotic cervical and upper thoracic vertebral lesions

sclerotic, or mixed in each patient and each region in a whole-body skeleton examination.

Chiabai et al [12] evaluated patients with solid cancers and multiple myeloma using T1WI, STIR combination, and T2-Dixon protocols showing approximately a sensitivity of more than 93% in both protocols and slightly higher specificity (difference +3%) in T1/STIR compared to T2-Dixon protocols in bone metastases detection regardless of the region.

Unlike, Lecouvet et al [19], who investigated the overall accuracy of T1 FSE only which was superior to T2-Dixon fat images yet did not include the STIR sequence (difference +4%,  $p < 0.0083$ ).

Our study correlated with that of Chiabai et al [12] with comparable sensitivity of both WB-MRI protocols with trivial superior sensitivity of T2-Dixon in lytic lesion detection and nearly similar sensitivity between both protocols in the detection of mixed lesions. On the other

**Table 4** Evaluation of image quality and artifacts. T1WI versus fat Dixon and STIR versus water Dixon

Category	T1WI	Percent	Fat Dixon	Percent	Equal	Percent
Motion artifact	5	0.17	23	0.77	2	0.07
Anatomic sharpness	2	0.07	26	0.87	2	0.07
CSF flow	4	0.13	5	0.17	21	0.70
Overall image quality	1	0.03	26	0.87	3	0.10
Category	STIR	Percent	Water Dixon	Percent	Equal	Percent
Motion artifact	0	0.00	27	0.90	3	0.10
Anatomic sharpness	0	0.00	21	0.70	9	0.30
CSF flow	1	0.03	3	0.10	26	0.87
Fat suppression	5	0.17	4	0.13	21	0.70
Overall image quality	0	0.00	27	0.90	3	0.10

The numbers represent the number of exams in which the observers selected the T1/STIR or water Dixon and fat Dixon images for the best quality or least amount of artifacts among the 30 patients in this study. If there was no difference between T1/STIR and water Dixon/fat Dixon images, they were scored as equivalent

**Table 5** The non-perfect agreement between junior and senior readers using weighted kappa values

STANDARD (T1,STIR)		$k_w$	95% CI	T2-Dixon (fat + water)		$k_w$	95% CI
Femurs	Lytic	0.84	0.66–1	Femurs	Lytic	0.9	0.76–1
Thoracic v	Lytic	0.94	0.81–1.1	Thoracic v	Lytic	0.94	0.81–1.06
	Sclerotic	0.88	0.68–1.08		Sclerotic	0.9	0.73–1.07
Thoracic cage	Sclerotic	0	0		Sclerotic	0.9	0.73–1.07
Humeri	Lytic	0.87	0.62–1.1	Humeri	Lytic	0.9	0.69–1.1
	Sclerotic	Insufficient			Sclerotic	Insufficient	
Skull	Lytic	Insufficient		Skull	Lytic	Insufficient	
	Sclerotic	Insufficient			Sclerotic	Insufficient	

hand, the specificity of both protocols in our study was approximately the same and consistently exceeded 95% across various anatomical regions and lesion types in comparison with the slightly higher specificity of T1WI, STIR combinations noted in Chiabai et al [12] study.

Moreover, our study showed very good inter-reader reliability for both T2-Dixon and T1WI-STIR sequences. Interestingly, the T2-Dixon sequence demonstrated superior quantitative inter-reader agreement between junior and senior readers. This was consistent with Hahn et al [17] who concluded that T2-Dixon water imaging exhibited the highest level of agreement, while T1-weighted imaging showed the lowest agreement, yet they did not include STIR sequences. Additionally, Chiabai et al [12] showed similar agreement between both readers regardless of the protocol and the region. This potentially supports that T2-Dixon imaging may offer better image quality and reduced reliance on the experience of radiologists for accurate lesion identification compared to T1-weighted or T1 + STIR sequences.

False positive results in both T1-STIR and T2 Dixon (fat + water) sequences were detected only in lytic lesions

in this study owing to benign conditions like enchondromas, hemangiomas, and degenerative changes. Similar pitfalls were recorded in previous published research [20]. False-negative results were more noticeable in sclerotic lesions, limiting their overall assessment on both T1+STIR and T2 Dixon sequences, which we assume might be attributed to the nature of low signal sclerotic lesions in all pulse sequences hindering contrast characteristics of the lesions displayed over the background bony marrow. Per-regionally, the thoracic cage region was the site of the highest false negative results which could be due to coronal images limiting the accurate assessment of this region.

Junior readers exhibited an overall higher prevalence of identifying false positive and false negative outcomes in T2-Dixon and T1-STIR sequences owing to their limited experience in the practice.

The total acquisition duration for the T2-Dixon sequence in this investigation was 6 min and 48 s, whereas the combined acquisition time for the T1WI and STIR amounted to 13 min and 44 s. This signified a noteworthy reduction, exceeding fifty percent, in

the overall time required for each patient study when employing the T2-Dixon sequence in comparison with the T1-STIR combination. Our acquisition timing correlated with Chiabai et al [12] who reported a significant reduction in time of approximately 40% when employing the T2-Dixon sequence compared to T1/STIR sequences. Similarly, Maeder et al [18] found a reduction of about 30% in acquisition time with T2-Dixon compared to T1WI sequences alone.

### Limitations

There were some limitations in our study. First, the images were assessed only qualitatively with no available software in our centers to measure values of signal-to-noise ratio and contrast-to-noise ratio. Additionally, we used a semiquantitative method in counting the number of metastatic bony lesions in each anatomical region in the study slightly limited the accuracy of the study. However, this was imperative for obtaining systematically organized data.

Second, lesions detected at the skull and humeri were too few among the patients which affected the results in these regions with a relatively overall small sample size in our study.

Third, our study was limited in sclerotic lesion detection as there were high false negative results as explained before.

At last, although histopathologic analysis typically acts as the established reference standard for bone metastases, it was impractical to obtain pathology for every lesion in our patient sample. Despite limited access to PET-CT and bone scintigraphy in our study population, we utilized a consensus reference standard involving close clinical monitoring and a variety of imaging modalities, aligning with the approach taken in the majority of similar prior studies.

### Conclusions

Our study indicated that an anatomical whole-body MRI (WB-MRI) protocol, centered on a single T2 Dixon sequence with fat and water reconstructions, can serve as a viable alternative to the reference T1 + STIR sequences for skeletal screening. This substitution resulted in a reduction in the examination duration without compromising either the quality or the imaging diagnostic accuracy.

### Abbreviations

ACC	Accuracy
CI	Confidence interval
CT	Computed tomography
DWI	Diffusion-weighted imaging
FN	False negative
FP	False positive
IP	In-phase

Kw	Weighted kappa
MSS	Matthews correlation coefficient
NPV	Negative predictive value
OP	Out-of-phase
PET	Positron emission tomography
PPV	Positive predictive value
Se	Sensitivity
Sp	Specificity
STIR	Short-tau inversion recovery
TI	Inversion time
TN	True negative
TP	True positive
TR/TE	Repetition time/time to echo
WB-MRI	Whole-body magnetic resonance imaging
2D T1 FSE	Two-dimension T1 fast spin echo sequence

### Supplementary Information

The online version contains supplementary material available at <https://doi.org/10.1186/s43055-024-01314-y>.

Supplementary Material 1: Table 1. Per-regional sensitivity and specificity of T1 + STIR and T2 Dixon for both junior (reader 1) and senior (reader 2) readers in each region

### Acknowledgements

We are grateful to Ahmed Fathy, Radiology Senior Technician at Mansoura University Hospitals, EG, who helped us in the scanning process of our patients and applying proper acquisition parameters.

### Author contributions

All authors have read and approved the manuscript. The study concept and design were proposed by ME and NM. Statistical analysis of data; MAH. Writing the original manuscript; ME and NM. Revision of the manuscript for important intellectual content; MAH & AS.

### Funding

This study had no funding from any resource.

### Availability of data and materials

The datasets used and/or analyzed during the current study are available from the corresponding author on reasonable request.

### Declarations

#### Ethics approval and consent to participate

This study was approved by the Research Ethics Committee of the Faculty of Medicine at Mansoura University in Egypt on 10/1/2023; reference number of approval: MS.22.12.2250.

#### Consent for publication

All patients included in this research gave written informed consent to publish the data contained within this study.

#### Competing interests

The authors declare that they have no competing interests.

Received: 26 April 2024 Accepted: 12 July 2024

Published online: 19 August 2024

### References

1. Dresen RC, De Vuysere S, De Keyzer F, Van Cutsem E, Prenen H, Vanslebrouck R, De Hertogh G, Wolthuis A, D'Hoore A, Vandecaveye V (2019) Whole-body diffusion-weighted MRI for operability assessment in

- patients with colorectal cancer and peritoneal metastases. *Cancer Imaging* 19(1):1–10. <https://doi.org/10.1186/s40644-018-0187-z>
2. Takahara T, Imai Y, Yamashita T, Yasuda S, Nasu S, Van Cauteren M (2004) Diffusion weighted whole body imaging with background body signal suppression (DWIBS): technical improvement using free breathing, STIR and high resolution 3D display. *Radiat Med* 22(4):275–282
  3. Walker R, Kessar P, Blanchard R, Dimasi M, Harper K, DeCarvalho V, Yucel EK, Patriquin L, Eustace S (2000) Turbo stir magnetic resonance imaging as a whole-body screening tool for metastases in patients with breast carcinoma: preliminary clinical experience. *J Magn Reson Imaging* 11(4):343–350. [https://doi.org/10.1002/\(SICI\)1522-2586\(200004\)11:4%3c343::AID-JMRI1%3e3.0.CO;2-P](https://doi.org/10.1002/(SICI)1522-2586(200004)11:4%3c343::AID-JMRI1%3e3.0.CO;2-P)
  4. Kwee TC, Kwee RM, Verdonck LF, Bierings MB, Nievelstein RA (2008) Magnetic resonance imaging for the detection of bone marrow involvement in malignant lymphoma. *Br J Haematol* 141(1):60–68. <https://doi.org/10.1111/j.1365-2141.2008.07020.x>
  5. Ghanem N, Lohrmann C, Engelhardt M, Pache G, Uhl M, Saueressig U, Kotter E, Langer M (2006) Whole-body MRI in the detection of bone marrow infiltration in patients with plasma cell neoplasms in comparison to the radiological Skeletal Survey. *Clin Imaging* 30(6):440–441. <https://doi.org/10.1016/j.clinimag.2006.08.018>
  6. Lauenstein TC, Goehde SC, Herborn CU, Goyen M, Oberhoff C, Debatin JF, Ruehm SG, Barkhausen J (2004) Whole-body MR imaging: evaluation of patients for metastases. *Radiology* 233(1):139–148. <https://doi.org/10.1148/radiol.2331030777>
  7. Albano D, Stecco A, Micci G, Sconfienza LM, Colagrande S, Reginelli A, Grassi R, Carriero A, Midiri M, Lagalla R, Galia M (2020) Whole-body magnetic resonance imaging (WB-MRI) in oncology: an Italian survey. *La Radiol Med* 126(2):299–305. <https://doi.org/10.1007/s11547-020-01242-7>
  8. Larbi A, Omoumi P, Pasoglou V, Michoux N, Triqueneaux P, Tombal B, Cyteval C, Lecouvet FE (2018) Whole-body MRI to assess bone involvement in prostate cancer and multiple myeloma: comparison of the diagnostic accuracies of the T1, short tau inversion recovery (STIR), and high B-values diffusion-weighted imaging (DWI) sequences. *Eur Radiol* 29(8):4503–4513. <https://doi.org/10.1007/s00330-018-5796-1>
  9. Lee K, Park HY, Kim KW, Lee AJ, Yoon MA, Chae EJ, Lee JH, Chung HW (2019) Advances in whole body MRI for musculoskeletal imaging: diffusion-weighted imaging. *J Clin Orthop Trauma* 10(4):680–686. <https://doi.org/10.1016/j.jcot.2019.05.018>
  10. Zormpas-Petridis K, Tunariu N, Curcean A, Messiou C, Curcean S, Collins DJ, Hughes JC, Jamin Y, Koh D-M, Blackledge MD (2021) Accelerating whole-body diffusion-weighted MRI with deep learning-based denoising image filters. *Radiol Artif Intell* 3(5):e200279. <https://doi.org/10.1148/ryai.2021200279>
  11. Pasoglou V, Michoux N, Larbi A, Van Nieuwenhove S, Lecouvet F (2018) Whole body MRI and oncology: recent major advances. *Br J Radiol* 91(1090):20170664. <https://doi.org/10.1259/bjr.20170664>
  12. Chiabai O, Van Nieuwenhove S, Vekemans M-C, Tombal B, Peeters F, Wuts J, Triqueneaux P, Omoumi P, Kirchgessner T, Michoux N, Lecouvet FE (2022) Whole-body MRI in oncology: Can a single anatomic T2 Dixon sequence replace the combination of T1 and STIR sequences to detect skeletal metastases and myeloma? *Eur Radiol* 33(1):244–257. <https://doi.org/10.1007/s00330-022-09007-8>
  13. Muger A, Suh KJ, Huisman TAGM, Weber K, Belzberg AJ, Carrino JA, Chhabra A (2013) Sclerotic lesions of the spine: MRI assessment. *J Magn Reson Imaging* 38(6):1310–1324. <https://doi.org/10.1002/jmri.24247>
  14. Nakanishi K, Tanaka J, Nakaya Y, Maeda N, Sakamoto A, Nakayama A, Satomura H, Sakai M, Konishi K, Yamamoto Y, Nagahara A, Nishimura K, Takenaka S, Tomiyama N (2021) Whole-body MRI: detecting bone metastases from prostate cancer. *Jpn J Radiol* 40(3):229–244. <https://doi.org/10.1007/s11604-021-01205-6>
  15. Altman DG (1990) *Practical statistics for medical research*. Chapman and Hall/CRC, Boca Raton. <https://doi.org/10.1201/9780429258589>
  16. Landis JR, Koch GG (1977) The measurement of observer agreement for categorical data. *Biometrics* 33(1):159–174. <https://doi.org/10.2307/2529310>
  17. Hahn S, Lee YH, Suh J-S (2018) Detection of vertebral metastases: a comparison between the modified Dixon turbo spin echo T2 weighted MRI and conventional T1 weighted MRI: a preliminary study in a tertiary center. *Br J Radiol* 91:20170782. <https://doi.org/10.1259/bjr.20170782>
  18. Maeder Y, Dunet V, Richard R, Becce F, Omoumi P (2018) Bone marrow Metastases: T2-weighted Dixon spin-echo fat images can replace T1-weighted spin-echo images. *Radiology* 286(3):948–959. <https://doi.org/10.1148/radiol.2017170325>
  19. Lecouvet FE, Pasoglou V, Van Nieuwenhove S, Van Haver T, de Broqueville Q, Denolin V, Triqueneaux P, Tombal B, Michoux N (2020) Shortening the acquisition time of whole-body MRI: 3D T1 Gradient Echo Dixon vs fast spin echo for metastatic screening in prostate cancer. *Eur Radiol* 30(6):3083–3093. <https://doi.org/10.1007/s00330-019-06515-y>
  20. Ohno Y, Koyama H, Onishi Y, Takenaka D, Nogami M, Yoshikawa T, Matsumoto S, Kotani Y, Sugimura K (2008) Non-small cell lung cancer: whole-body mr examination for M-stage assessment—utility for whole-body diffusion-weighted imaging compared with integrated FDG PET/CT. *Radiology* 248(2):643–654. <https://doi.org/10.1148/radiol.2482072039>

## Publisher's Note

Springer Nature remains neutral with regard to jurisdictional claims in published maps and institutional affiliations.